

# 1 Treatment of Glyphosate-Contaminated Water for Sustainable Environmental Management

2 Imene Feddal <sup>1,2\*</sup>, Goussef Mimanne<sup>2</sup>, Sihem Nehal<sup>3</sup>

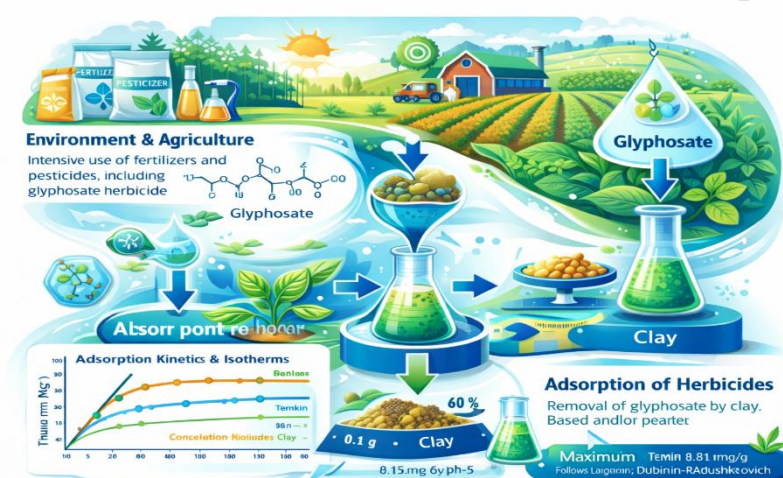
3 <sup>1</sup>Faculty of Science and Technology, Abdel Hamid Ibn Badis University of Mostaganem, 27000

4 <sup>2</sup>Laboratory of Materials & Catalysis, Faculty of Exact Sciences Djillali LIABES University (UDL)

5 <sup>3</sup>Djillali Liabes University of Sidi Bel Abbas 22000

6 \*Corresponding author: [fimene22@hotmail.com](mailto:fimene22@hotmail.com)

## 7 Graphical abstract



8

9

10 **Abstract.**

11 The natural environment is defined as the entirety of the Earth's natural components and has been  
12 increasingly impacted by human activities in recent decades. Agricultural intensification, particularly  
13 in Algeria, has led to a substantial increase in the use of fertilizers and phytosanitary products to  
14 improve crop yield and quality. Among these products, glyphosate is the most widely used herbicide  
15 for weed control due to its effectiveness against annual, biennial, and perennial plants. This study  
16 investigates the removal of glyphosate from contaminated water using an abundant natural material,  
17 sodium-modified clay. Physicochemical characterizations were carried out to identify the surface  
18 functional groups and charge properties of the adsorbent. Adsorption experiments demonstrated that  
19 a clay mass of 0.1 g removed approximately 60% of glyphosate within 20 min at pH 5. Kinetic  
20 analysis showed that the adsorption process follows a pseudo-second-order model. Adsorption  
21 isotherm studies were conducted to elucidate the adsorption mechanism. The experimental data fitted  
22 well with the Langmuir, Temkin, and Dubinin–Radushkevich models, indicating monolayer  
23 adsorption with a maximum adsorption capacity of 18.18 mg g<sup>-1</sup>. These results highlight the potential  
24 of sodium clay as an efficient, low-cost adsorbent for glyphosate removal from contaminated water.

25 **Keywords:** Environment, Agronomy, adsorption, herbicide, Clay.

26  
27 **1. Introduction**

28 Environmental pollution, particularly the contamination of water resources by chemical substances,  
29 has become one of the most pressing global challenges of the twenty-first century. Rapid  
30 industrialization, intensified agricultural practices (Altenor et al., 2009; Baghdadi et al., 2017;  
31 Elaziouti et al., 2011; Amari et al., 2018), and demographic growth have significantly increased the  
32 release of hazardous compounds into aquatic environments (Al-Muhtase et al., 2011; Ugurlu et al.,  
33 2011; Gong et al., 2011; Maldonado et al., 2006). Water, an essential resource for human life, food  
34 production, and economic development, is increasingly exposed to degradation due to anthropogenic  
35 activities (Aysegul et al., 2013). Among the various sources of contamination, agricultural runoff

36 represents a major contributor to diffuse pollution, especially through the widespread use of pesticides  
37 and herbicides (Lunhong et al., 2011; Barka et al., 2008; Zhang et al., 2013). Herbicides are  
38 extensively applied worldwide to enhance agricultural productivity by controlling weeds and  
39 protecting crops. However, their intensive and sometimes uncontrolled use has led to serious  
40 environmental and health concerns (Mansour et al., 2011; Omer et al., 2018; Khan et al., 2019;  
41 Medjdoubi et al., 2019). Once introduced into the environment, these compounds can persist in soil  
42 and migrate into surface and groundwater systems through leaching and runoff processes. Even at  
43 low concentrations, the presence of herbicides in water bodies may pose risks to aquatic ecosystems  
44 and human health (Zhang et al., 2013; Altenor et al., 2009).

45 Glyphosate (N-(phosphonomethyl)glycine) is one of the most widely used non-selective herbicides  
46 globally. It is employed in a variety of agricultural systems, including cereal crops, orchards,  
47 vineyards, and vegetable production, as well as in non-agricultural settings. Despite its effectiveness  
48 in weed control, glyphosate has become a subject of intense scientific debate due to its potential  
49 toxicity and environmental persistence (Bentahar et al., 2018; Hu et al., 2018; Boukhemkhem et al.,  
50 2017). Several studies have reported its detection in rivers, groundwater, and even drinking water  
51 sources. Moreover, its classification as a probable carcinogenic compound by international agencies  
52 has heightened public and regulatory concern. As a consequence, the development of efficient and  
53 economically viable methods for glyphosate removal from contaminated water has become a priority  
54 in environmental research (Mouni et al., 2018; Ngulube et al., 2017; Sarma et al., 2011). Various  
55 physical, chemical, and biological treatment technologies have been proposed to reduce pesticide  
56 concentrations in wastewater, including advanced oxidation processes, membrane filtration,  
57 biodegradation, and coagulation–flocculation techniques (Kausar et al., 2018; Şahin et al., 2015).  
58 Among these methods, adsorption has emerged as one of the most effective and widely applied  
59 approaches due to its operational simplicity, high removal efficiency, and relatively low cost. Recent  
60 studies have reported the effective removal of glyphosate using natural and modified clay materials,  
61 highlighting the importance of adsorption mechanisms and surface interactions (Magda et al., 2026;

62 Osama et al., 2022; Sabrina et al., 2022; Sabiha et al., 2025). The principle of adsorption is based on  
63 the accumulation of pollutant molecules onto the surface of a solid material, known as an adsorbent,  
64 through physical or chemical interactions. Activated carbon is traditionally considered one of the  
65 most efficient adsorbents; however, its relatively high cost and regeneration requirements limit its  
66 large-scale application, particularly in developing regions. Consequently, increasing attention has  
67 been directed toward low-cost and naturally abundant materials. Natural clays have attracted  
68 significant interest in this context due to their availability, environmental compatibility, and favorable  
69 physicochemical properties. In particular, sodium-rich smectitic clays are widely distributed across  
70 many regions of the world and exhibit similar structural and surface characteristics. These clays are  
71 characterized by a layered structure, high specific surface area, notable swelling capacity, and  
72 substantial cation exchange capacity. Their negatively charged surfaces and exchangeable interlayer  
73 cations enable various interaction mechanisms with ionic and polar contaminants. Such intrinsic  
74 properties make sodium smectitic clays promising candidates for the adsorption of herbicides such as  
75 glyphosate, which possesses multiple functional groups capable of participating in electrostatic  
76 interactions, hydrogen bonding, and surface complexation reactions.

77 Although numerous studies have investigated the adsorption of pesticides onto different materials,  
78 including activated carbon, zeolites, and modified biomaterials, the adsorption behavior of glyphosate  
79 onto sodium-rich natural smectitic clays remains insufficiently explored in a comprehensive manner.  
80 Existing works often focus on removal efficiency without providing an integrated mechanistic  
81 analysis combining adsorption kinetics, equilibrium modeling, and systematic evaluation of  
82 operational parameters. Furthermore, while some studies have examined specific clay samples, the  
83 broader applicability of findings to widely distributed clay categories have not always been clearly  
84 emphasized. It is important to underline that sodium smectitic clays are not restricted to a single  
85 geographical location. They belong to a mineralogical family that is globally available and shares  
86 comparable physicochemical characteristics across different regions. Therefore, investigating the  
87 adsorption behavior of a locally sourced sodium clay provides insights that are transferable to similar

88 materials worldwide. The adsorption mechanisms governing glyphosate removal are primarily  
89 determined by the structural and chemical properties of the clay mineral rather than by its  
90 geographical origin. Understanding these mechanisms is essential for designing efficient and  
91 sustainable water treatment strategies. In this context, the present study aims to investigate the  
92 adsorption performance of a sodium natural clay toward glyphosate removal from aqueous solutions.  
93 Although the clay sample used in this work was locally collected, it is representative of a widely  
94 distributed smectitic clay family, thereby ensuring the broader relevance of the results. The study  
95 focuses on enhancing adsorption performance through a simple and cost-effective pretreatment  
96 method, making the approach practical and economically feasible. The proposed treatment process is  
97 designed as a pre-irrigation remediation step, intended to improve the quality of contaminated  
98 groundwater before its agricultural use, thereby reducing environmental and food-chain transfer risks.  
99

100 A comprehensive parametric investigation was conducted to evaluate the influence of key operational  
101 variables, including contact time, adsorbent dosage, pH of the solution, and initial glyphosate  
102 concentration. Adsorption kinetics were analyzed using pseudo-first-order and pseudo-second-order  
103 models, as well as the intraparticle diffusion model, to identify the rate-controlling mechanisms. In  
104 addition, equilibrium data were interpreted through isotherm models in order to elucidate the  
105 adsorption behavior and determine the interaction characteristics between glyphosate molecules and  
106 the clay surface. By integrating kinetic modeling, equilibrium analysis, and operational parameter  
107 optimization, this work provides a detailed mechanistic understanding of glyphosate adsorption onto  
108 sodium smectitic clays. The originality of the study lies in the combination of a low-cost enhancement  
109 strategy with a comprehensive analytical approach applied to a clay type that is globally distributed.  
110 The findings contribute to advancing knowledge on glyphosate–clay interactions and support the  
111 development of sustainable, accessible, and scalable water treatment solutions beyond a strictly local  
112 framework. The originality of this study lies in the combination of a low-cost and easily applicable  
113 pretreatment strategy with a comprehensive mechanistic analysis of glyphosate adsorption onto a

114 widely available sodium smectitic clay. This approach provides both fundamental insights and  
115 practical relevance for sustainable water treatment applications.

## 116 2. Experimental

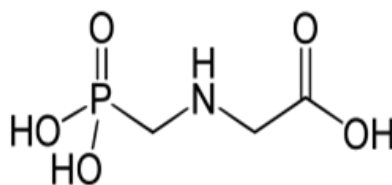
### 117 2.1. Materials

118 The adsorbent used is bentonite coming from the deposit of ghousel "Hammam Bouhrara," located  
119 in the west of Algeria. To improve its adsorption capacity, we subjected the bentonite to a chemical  
120 treatment. This operation consists in removing the impurities found in the clay, such as organic  
121 matter, iron sulfides formed, and aluminum hydroxides and oxides. The clay is chemically treated  
122 with HCl (0.5M) and hydrogen peroxide (H<sub>2</sub>O<sub>2</sub>). After each operation, the clay pellet is filtered and  
123 then washed until the total elimination of chlorides (silver nitrate test). Then we proceed to the  
124 saturation with sodium, carried out to ensure homogenization of the clay. This is done by exchange  
125 with a solution of NaCl (1N). The operation is repeated 3 times with distilled water and then a wash  
126 until the supernatant does not contain any chlorides.

### 127 2.2. Adsorbate

128 Glyphosate N-(phosphonomethyl) Glycine is a synthetic molecule, a weak organic acid analog of a  
129 natural amino acid, absorbed by the leaves. It is very soluble in water and very polar and soluble in  
130 most organic solvents (Organisation mondiale de la santé (OMS), 2025) (Figure 1).

131



132

133

**Figure 1.** The molecule of Glyphosate.

134

135

136

137

### 138 2.3. Instruments

139 Fourier transform infrared (FTIR) spectroscopy was performed using a PerkinElmer ALPHA Bruker  
140 spectrometer equipped with an attenuated total reflectance (ATR) diamond crystal. Spectra were  
141 recorded over the wavenumber range of 4000–400  $\text{cm}^{-1}$  in order to identify the surface functional  
142 groups and chemical structure of the adsorbent material. The mineralogical composition and  
143 crystalline structure of the clay were analyzed by X-ray diffraction (XRD) using a Philips Analytical  
144 X'PERT Pro diffractometer with Cu  $K\alpha$  radiation ( $\lambda = 1.5418 \text{ \AA}$ ), operating at 45 kV and 40 mA. The  
145 data were collected over an appropriate  $2\theta$  range with a scanning time of 10–20 minutes. The point  
146 of zero charge ( $\text{pH}_{\text{pzc}}$ ) of the adsorbent was determined using the pH drift method, as described in  
147 previous work (Imene et al., 2019), in order to evaluate the surface charge properties of the material.

### 149 2.4. Adsorption study

150 All experiments are done at room temperature ( $25^\circ\text{C}$ ); the protocol is as follows: A known mass of  
151 clay is suspended in a known volume of a solution of glyphosate at the desired concentration; the  
152 suspensions are then shaken and then filtered; the glyphosate remaining in equilibrium is analyzed  
153 by UV-visible spectrometry. Concerning our work, we have realized first the influence of various  
154 experimental parameters, then the adsorption kinetics to determine the adsorption mechanism  
155 between the support and the glyphosate solution at equilibrium. All experiments were performed in  
156 triplicate, and the results are expressed as mean  $\pm$  standard deviation (SD). The adsorbed quantities  
157 are calculated using the following equation:

$$158 \quad Q_{\text{ads}} = \frac{C_0 - C_{\text{eq}}}{m} \cdot V \quad (1)$$

159 And the percentage of discoloration is calculated as follows:

$$160 \quad P(\%) = \frac{C_0 - C_{\text{eq}}}{C_0} \cdot 100 \quad (2)$$

161 With:  $Q_{\text{ads}}$ : Adsorbed quality by a gram of the adsorbent in (mg/g),  $C_0$ : initial concentration in  
162 (mg/L),  $C_{\text{eq}}$ : concentration at equilibrium in (mg/L),  $V$ : Solution volume in (L),  $m$ : Adsorbent mass  
163 in (g),  $P(\%)$ : Percentage of discoloration.

164 The results obtained from the protocols followed in the laboratory are given in curves for each  
165 parameter: the contact time, the pH of the solution, the mass of clay in the solution, and the influence  
166 of the initial concentration. Statistical analysis was performed using one-way ANOVA at a 95%  
167 confidence level ( $p < 0.05$ ). All experiments were conducted in triplicate.

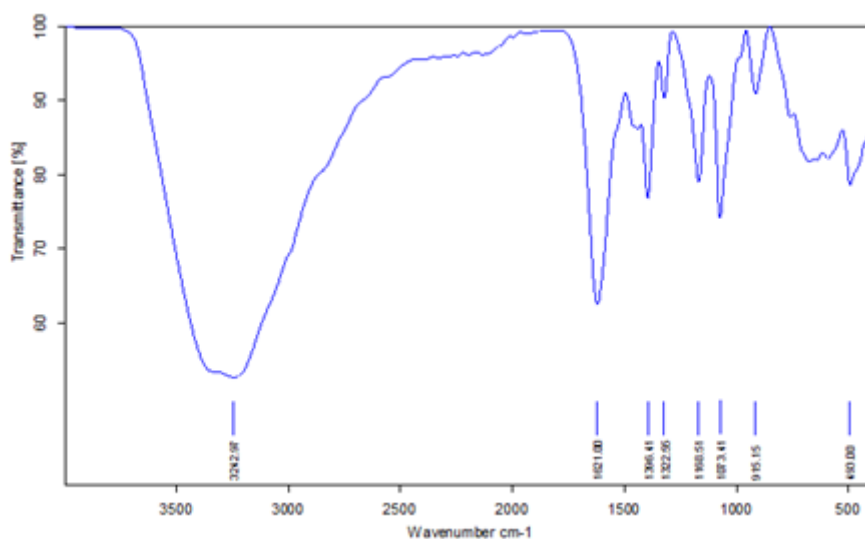
### 168 **3. Results and discussion**

#### 169 **3.1.Characterization of the materials**

170 According to the table of infrared spectroscopy, For the spectrum of glyphosate (Figure 2), we  
171 observe a band located at  $3242\text{ cm}^{-1}$ ; this band is attributed to the vibration of elongation of the OH  
172 bond. And the band located at  $1621\text{ cm}^{-1}$  corresponds to the elongation of the bond C=O. The band  
173 located at  $1396\text{ cm}^{-1}$  corresponds to a deformation in the OH bond plane. The band located at  $1322$   
174  $\text{cm}^{-1}$  is attributed to the C-N amine function, and the band located at  $1166\text{ cm}^{-1}$  is due to the CO<sub>2</sub>H  
175 acid bond. And lastly, the band is located at  $1073\text{ cm}^{-1}$ , which is due to the elongation of the N-H  
176 bond. For the FTIR spectrum concerning the sodium clay (Figure 3), an intense band located between  
177 900 and 1200, centered around  $1040\text{ cm}^{-1}$ , corresponds to the valence vibrations of the Si-O bond.  
178 The bands located at 525, 466, and  $422\text{ cm}^{-1}$  are attributed, respectively, to the deformation vibrations  
179 of Si-O-Al bonds and Si-O-Mg and Si-O-Fe bonds. Also, characteristic bands of Al-OH deformation  
180 vibrations appear between  $770$  and  $800\text{ cm}^{-1}$ . The sharing of the OH group between Fe and Al atoms  
181 in octahedral position can shift the Al-OH vibrations to about  $680$  and  $794\text{ cm}^{-1}$ . The Mg-O and Mg-  
182 OH vibrations (confused with Si-O) are located at  $515$  and  $490\text{ cm}^{-1}$ , respectively. The band located  
183 at  $3415\text{ cm}^{-1}$  is due to the elongation of the OH bond, and the band located at  $1622\text{ cm}^{-1}$  is attributed  
184 to the elongation of the C=O bond.

185

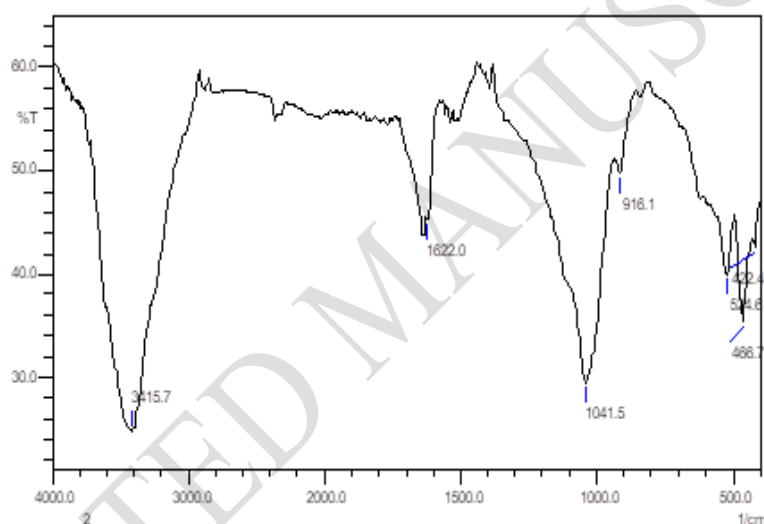
186



187

188

**Figure 2.** FTIR spectra of glyphosate.



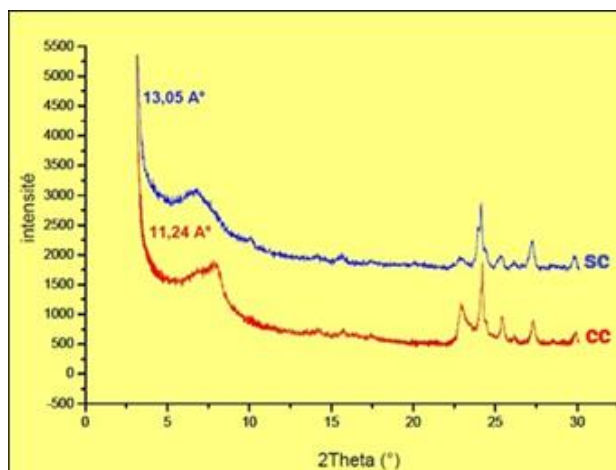
189

190

**Figure 3.** FTIR spectra of sodium clay.

191 XRD examination confirms the good purification of the clay since impurities such as quartz (3.88 Å),  
 192 calcite (3.68 Å), and cristobalite 3.50 Å are largely eliminated during purification (Figure 4). We also  
 193 note that there is an increase in the basal distance for the clay; it goes from 11.24 Å for the raw clay  
 194 (CC) to 13.05 Å for the sodium clay (SC).

195



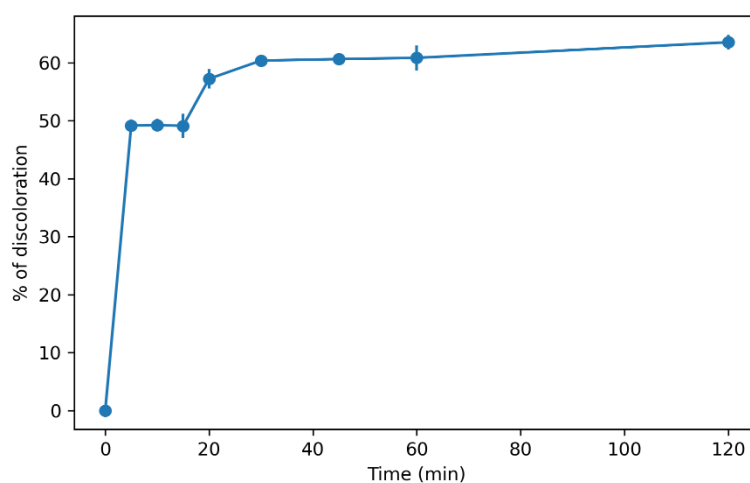
196  
197 **Figure 4** . Diffractogramm of raw and sodium clays.

198 The specific surface of raw and sodium clay is 42 m<sup>2</sup>/g and 96 m<sup>2</sup>/g, respectively, which confirms the  
199 good purification of our clay. The pHZPC value for sodium clay is 5.11; i.e., for pH values above  
200 pHZPC, the surface of our material is negatively charged, and for pH values below pHZPC, the  
201 surface is positively charged (Guiza el al. 2013, Youcef et al. 2006, Benguella el al. 2006).

202 **3.2.Adsorption of glyphosate**

203 **3.2.1. Effect of contact time**

204 The first test was performed with a concentration of 10 g/L under agitation at different times. The  
205 result of this test is represented in this case graphically by the percentage of discoloration as a  
206 function of contact time (Figure 5).



207

208 **Figure 5.** Effect of contact time on glyphosate removal efficiency using sodium natural clay. Error  
209 bars represent ± standard deviation of triplicate experiments.  
210

211 Figure 5 shows a rapid increase in the elimination of glyphosate on the sodium clay with increasing  
212 contact time. Elimination of the herbicide was observed from the first time; after a sufficient contact  
213 time of 20 min, the residual concentration of glyphosate in the aqueous phase decreased. As shown  
214 in Figure 1, the discoloration efficiency increased rapidly during the first 20 min, reaching  $57.23 \pm$   
215  $1.63\%$ . After 30 min, the process reached a plateau around 60%, indicating that equilibrium was  
216 achieved. This elimination is very fast at the first contact because of the availability of the active sites  
217 in our adsorbent. The rate of adsorption becomes stable after 20 min of agitation and reaches the  
218 equilibrium with a rate of 60%. This equilibrium is due to the saturation of the majority of the sites  
219 by the glyphosate. One-way ANOVA confirmed that contact time had a statistically significant effect  
220 on glyphosate removal efficiency ( $p < 0.05$ ), indicating that the observed differences between contact  
221 times are not due to random variation but reflect a true adsorption trend.

222

223

### 224 **3.2.2. Effect of pH solution**

225 The pH is an important factor in any adsorption study; it allows us to have and choose the best pH  
226 conditions for a charged molecule removal study and thus to minimize the number of experiments for  
227 a better adsorption capacity. In addition, to study the influence of pH on the adsorption of glyphosate  
228 on sodium montmorillonite, we prepared a solution of glyphosate with a concentration of 10 mg/L  
229 (the initial pH of the solution is 5). We then varied the pH of this solution between 2 and 10 using  
230 solutions of HCl and NaOH.

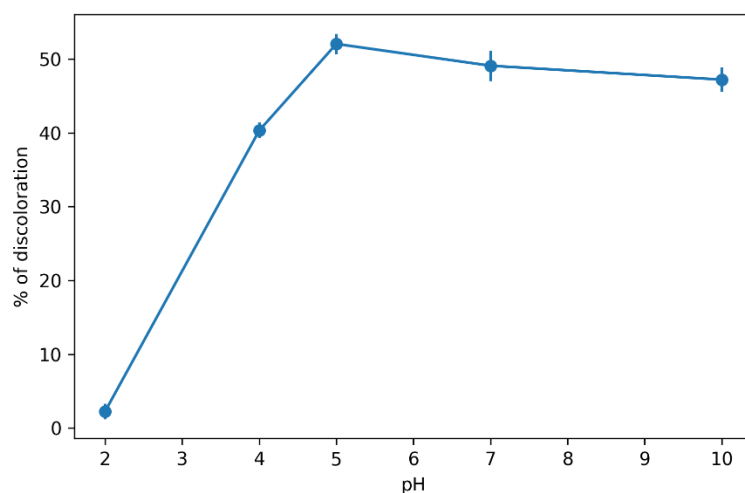


**Figure 6.** Effect of the pH on glyphosate adsorption onto sodium clay. Error bars represent  $\pm$  standard deviation of triplicate experiments.

Error bars represent the standard deviation of three independent experiments ( $n = 3$ ).

Figure 6 shows the effect of the pH of the solution on the adsorption capacity of glyphosate on sodium clay. It was found that the percentage of adsorption increased significantly with increasing pH until reaching a maximum (62%) at pH = 5 (initial pH of the solution of glyphosate). Figure 6 shows the effect of pH on discoloration efficiency. The removal efficiency increased from acidic pH to reach a maximum at pH 5 ( $52.07 \pm 1.38\%$ ), followed by a slight decrease at higher pH values. This result is confirmed by the study of pHZPC. At  $\text{pH} < \text{pHZPC}$ , the surface of the adsorbent is positively charged, which produces an attraction of the positively charged sites of the clay with the basic functions of glyphosate. The optimum pH is 5. ANOVA analysis confirmed that the differences in adsorption capacity between the different pH levels were statistically significant ( $p < 0.05$ ).

### 3.2.3. Influence of the adsorbent mass

Subsequently, the effect of adsorbent mass on the adsorption of glyphosate on sodium clay was tested; the result is shown in Figure 7.

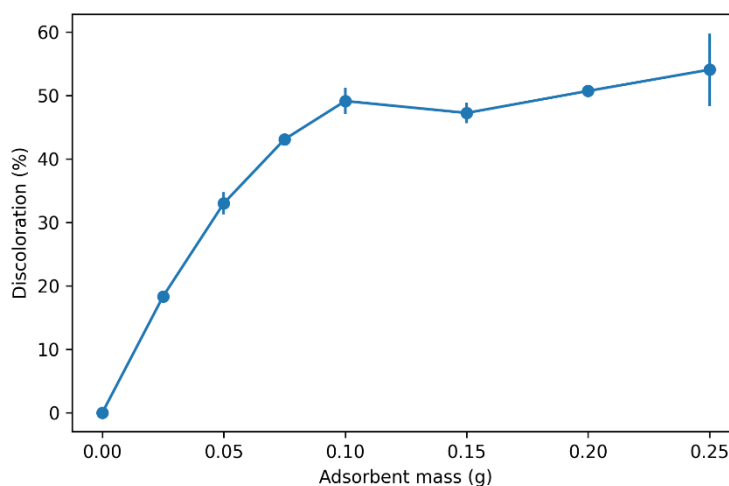


**Figure 7.** Effect of the adsorbent mass on glyphosate adsorption. Error bars represent  $\pm$  standard deviation of triplicate experiments.

248

249

250

251

252

253

254

255

256

257

258

259

260

261

262

263

264

The result presented in figure 7 shows that the adsorption rate of glyphosate increases from 18% to 52%; this is due to the presence of more active sites on the surface of the clay. The initial rapid increase is due to the availability of a larger surface area of the adsorbent, but a further increase in clay saturates the surface of the adsorbent, and equilibrium is reached. As shown in Figure 7. A mass of clay of 0.1 g is required to bind the maximum of glyphosate. Analysis of variance (ANOVA) confirmed that the differences in adsorption capacity between the different masses were statistically significant ( $p < 0.05$ ). Similar statistically significant effects were observed for adsorbent dose and contact time. The error bars in Figures 5, 6 and 7 represent the standard deviation ( $\pm$ ) calculated from three experiments performed in triplicate.

### 3.3.Isotherm study

This test concerns the effect of concentration on the adsorption of glyphosate on sodium montmorillonite; the results are shown in figure 8.

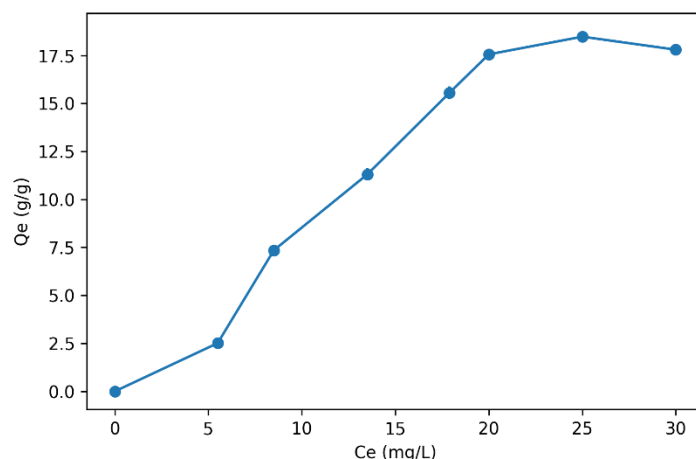


**Figure 8.** Adsorption isotherm of glyphosate onto sodium clay

Error bars represent the standard deviation of three independent experiments ( $n = 3$ ).

265

266

267

268

269 The plot of the figure above shows that the adsorption capacity increases with the increase of the  
 270 initial concentration. The isotherm presents an equilibrium level indicating the saturation of the  
 271 surface sites and thus the formation of a monolayer. Sodium montmorillonite has an adsorption  
 272 capacity of 18.18 g/g.

### 273 3.3.1. Modeling of adsorption isotherms

274 To better understand the adsorption process of glyphosate by sodium clay, the adsorption isotherm  
 275 data were analyzed based on several mathematical models widely used in the literature; the linear  
 276 forms of the models used are given in Table I (Mekatel et al. 2015, Rytwo et al. 2010, Chen et al.  
 277 2022).

278 Table I. Linear forms of the isotherm models used.

Models	Equation	Parameters
Freundlich	$\ln q_e = \ln K_F + \frac{1}{n} \ln C_e$	$q_e$ : quantity of solute adsorbed per unit mass of the adsorbent at equilibrium (mg/g). $K_F$ : Freundlich constant associated with the adsorption capacity. $C_e$ is the equilibrium concentration (mg/L)
Langmuir (mg/g). adsorption	$\frac{1}{q_e} = \frac{1}{C_e} \frac{1}{q_m K_L} + \frac{1}{q_m}$	$q_m$ : represents the maximum adsorption capacity  $K_L$ : equilibrium constant, equal to the ratio of and desorption rates (L/mg).

Temkin	$Q_e = B_T \ln K_T + B_T \ln C_e$	$K_T$ and $B_T$ : Temkin findings . $\Theta$ : the recovery rate
	$B_T = \frac{Q_m \cdot RT}{\Delta Q}$	
Elovich	$q_t = \frac{1}{\beta} \ln(\alpha\beta) + \frac{1}{\beta} \ln t$	$t$ : the time (min) $K_E$ : the equilibrium constant of Elovich (L/mg). $\alpha, \beta$ elovich constants
Dubini – Radushkevich	$\ln Q_e = \ln Q_{mDR} - K_D \cdot \epsilon^2$	$\epsilon$ : filling rate $K_D$ : constant Dubinin-Radushkevich
	$\epsilon = RT \ln\left(\frac{1}{1+C_e}\right)$ $E = \frac{1}{\sqrt{2} K_D}$	free energy

279

280 According to the results presented in table 2, the adsorption of glyphosate on sodium clay follows the  
 281 Langmuir model with  $R^2$  higher than 0.9 and  $q_{exp}$  and  $q_m$  close to each other; the value of  $R_L$  is  
 282 within the range of validity, confirming that the adsorption is favorable and takes place in a  
 283 monolayer. Temkin's model indicates that the adsorption of glyphosate on sodium clay is  
 284 chemisorption ( $R^2 > 0.9$ ). The Dubini-Radushkevich model allows us to calculate the average free  
 285 energy  $E$ , defined as the change of free energy when 1 mole of ion is transferred towards the surface  
 286 of the solid (if  $E < 8$  kJ/mol, it is a chemisorption, and if  $E > 8$  kJ/mol, the adsorption is physical). In  
 287 our case,  $E$  kJ/mol confirms the chemical nature of the adsorption of the glyphosate on the sodium  
 288 clay.

289 **Table 2.** Values of the parameters of the different equations studied

Models	Constants	Values
Freundlich	$R^2$	0.876
	$1/n$	0.220
	$K_F$ (mg.g <sup>-1</sup> )(L.mg <sup>-1</sup> )	2.34
Langmuir	$R^2$	0.938
	$q_m$ (mg.g <sup>-1</sup> )	18.18
	$K_L$ (L.mg <sup>-1</sup> )	0.27
	$R_L$	0.543
Temkin	$R^2$	0,926
	$K_T$ (L.mg <sup>-1</sup> )	4,22
	$B_T$ (KJ.mg <sup>-1</sup> )	3.939

Elovich	R <sup>2</sup> q <sub>m</sub> (mg.g <sup>-1</sup> ) K <sub>E</sub> (L.mg <sup>-1</sup> )	0.527 38.46 0,027
Dubini – Radushkevich	R <sup>2</sup> K <sub>D</sub> (mol <sup>2</sup> .J <sup>2</sup> ) Q <sub>mDR</sub> (mg.g <sup>-1</sup> ) E (KJ/mol)	0.968 .6*10 <sup>-6</sup> 16.91 0,00917

290

### 291 3.4.Kinetic study

292 In this part, different models of adsorption kinetics were tested to elucidate the mechanism of  
 293 adsorption in these microparticles. The models used in this study are the kinetics of the pseudo-first-  
 294 order (eq3) and second-order (eq4) as well as the intraparticle diffusion (eq5). These mathematical  
 295 models were chosen on the one hand for their simplicity and on the other hand for their application  
 296 in the field of adsorption of organic compounds on the various adsorbents.

$$297 \ln(q_e - q_t) = \ln q_e - k_1 t \quad (3)$$

$$298 \frac{t}{qt} = \frac{1}{K_2 qe^2} + \frac{t}{qe} \quad (4)$$

$$299 q_t = k_{int} t^{1/2} + C \quad (5)$$

300 Where Q<sub>e</sub> is the quantity of the adsorbed coloring in the equilibrium time (mg/g), Q<sub>t</sub> is the quantity  
 301 of the adsorbed coloring in the time t (mg/g), K<sub>1</sub> is the speed constant of the first class (min<sup>-1</sup>), K<sub>2</sub> is  
 302 the constant of the second-order speed (g/mg min), and h = K<sub>2</sub>. q<sub>e2</sub>, the initial diffusion speed (mg/g  
 303 min), C: ordinate originally, K<sub>int</sub>: the speed constant of intraparticle diffusion.

304 After analyzing the modeling results mentioned in the table below, we can conclude that the most  
 305 representative model of the adsorption kinetics is the second-order model, where the coefficient of  
 306 determination is 0.999, thus rapid adsorption. The pseudo-second-order model reveals that adsorption  
 307 is chemical and that adsorption depends on the adsorbent-adsorbate couple. We can therefore  
 308 conclude that the interaction between glyphosate and sodium clay occurs either by charge  
 309 neutralization or by electrostatic attraction. In conclusion, we can say that the adsorption of

310 glyphosate on sodium clay follows the pseudo-second-order model with intraparticle diffusion  
311 (Medjdoubi et al. 2019, Mouni et al. 2018).

312 It is important to note that, in real wastewater systems, the presence of co-existing pollutants such as  
313 other pesticides, heavy metal ions, and dissolved organic matter may influence glyphosate adsorption  
314 behavior. These species can compete with glyphosate for active adsorption sites, reduce adsorption  
315 efficiency through site blockage, or alter the surface properties of the adsorbent. In particular,  
316 dissolved organic matter may form complexes with glyphosate or occupy adsorption sites, thereby  
317 limiting its removal. Although the present study was conducted under controlled conditions using  
318 model aqueous solutions to better understand the adsorption mechanisms, these results provide a  
319 fundamental basis for predicting behavior in more complex systems. Further studies involving real  
320 wastewater matrices are necessary to fully evaluate the performance of the proposed adsorbent under  
321 practical conditions.

322

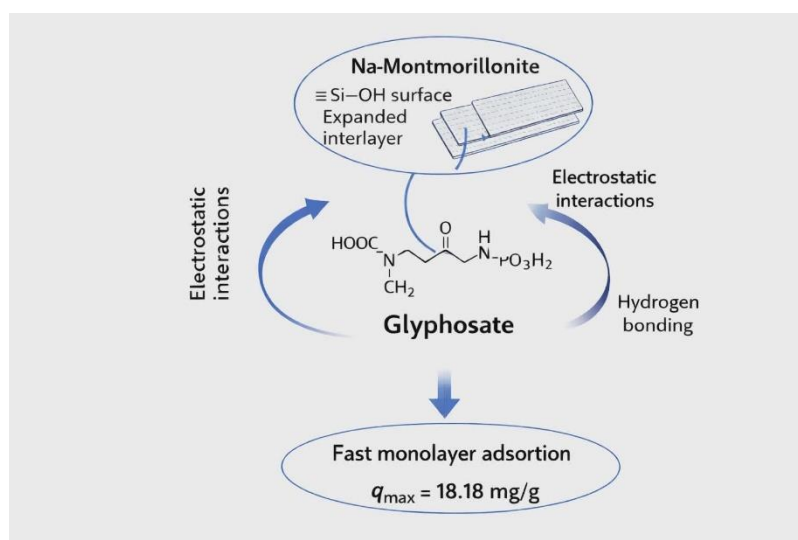
323 **Table 3.** Kinetic parameters of glyphosate adsorption on sodium clay

Adsorbent	Pseudo Premier Order			Pseudo second Order			Diffusion Intraparticulaire		
	Qe (mg/g)	K <sub>1</sub> (min <sup>-1</sup> )	R <sup>2</sup>	Qe (mg/g)	K <sub>2</sub> ((g mg <sup>-1</sup> .min <sup>-1</sup> )	R <sup>2</sup>	K <sub>diff</sub> (mg.g <sup>-1</sup> .min <sup>-1/2</sup> )	C	R <sup>2</sup>
Sodium Clay	06.61	-0.0006	0.855	3.41	0.1	0.999	0.312	9.35	0.914

324

#### 325 4. Glyphosate adsorption mechanism

326 The adsorption mechanism of glyphosate onto sodium clay is primarily governed by electrostatic  
327 interactions and hydrogen bonding (Figure 9). Under acidic to neutral pH conditions, glyphosate  
328 predominantly exists in an anionic form, which favors electrostatic attraction with positively charged  
329 sites and exchangeable sodium ions on the clay surface. Hydrogen bonding may also occur between  
330 the silanol (Si-OH) groups of montmorillonite and the functional groups of glyphosate, particularly  
331 the phosphonate and carboxylate groups. Furthermore, intraparticle diffusion plays a role in the  
332 adsorption process by facilitating the migration of glyphosate molecules into the interlayer spaces of  
333 the clay. These combined interactions lead to a stable monolayer adsorption mechanism, in agreement  
334 with Langmuir-type isotherm behavior (Yudha et al. 2025).



335  
336 **Figure 9.** Mechanism of glyphosate removal by sodium clay

337 **5. CONCLUSION**

338 This study had the objective, of the use of a natural material abundant in our country: the clay  
 339 chemically modified to increase its capacity of adsorption for the elimination of a herbicide very used  
 340 in Algeria: the glyphosate remaining in the agricultural wastewater. The physicochemical analyses  
 341 on the sodium clay showed the increase of the specific surface by the method of BET from 42m<sup>2</sup>/g  
 342 before treatment to 96m<sup>2</sup>/g for the sodium clay, the good insertion of sodium was also confirmed by  
 343 the increase of the basal distance from 11,24 Å to 13,05 Å. The adsorption process took place through  
 344 an interaction between the silanol groups of the montmorillonite and the studied herbicide, this  
 345 adsorption is influenced by the pH of the solution. The experimental results confirmed that the sodium  
 346 clay has an affinity towards glyphosate, after optimization of the parameters influencing the  
 347 adsorption, the maximum adsorption capacity is 18.18 mg/g and is done in monolayer, and the kinetic  
 348 study revealed that the adsorption is fast of order 2 with an intraparticle diffusion. Due to the vast  
 349 availability of clays in our country and the simplicity of processing, it is expected to have a significant  
 350 impact on the fate of herbicides in the environment. Although the proposed approach does not  
 351 introduce a novel adsorption material, it offers a practical and scalable solution based on naturally  
 352 abundant resources, combined with a detailed understanding of adsorption mechanisms, which is  
 353 essential for real-world water treatment applications.

354 **DECLARATION OF COMPETING INTEREST**

355 The authors declare that they have no conflict of interest.

356 **ACKNOWLEDGEMENTS**

357 The Algerian Directorate General of Scientific Research and Technological Development  
358 (DGRSDT), the Algerian Ministry of Higher Education and Scientific Research (MESRS), are greatly  
359 thanked.

360

361 **REFERENCES**

362 Al-Muhtase, A. H., Ibrahim, K. A., Albadrin, A.B., Ali-Khashman, O.,& Ahmad, M. N. (2011).  
363 Remediation of phenol- Contaminated Water by Adsorption Using Poly (Methyl Methacrylate)  
364 (PMMA), *Chemi. Engine. J.*, 168, 691-699.

365

366 Altenor, S., Carene, B., Emmanuel, E., Lambert, J., Ehrhardt, J. J.,Gaspard, S. (2009) Adsorption  
367 studies of methylene blue and phenol onto vetiver roots activated carbon prepared by chemical  
368 activation, *J. Hazard. Mater.* 1029–1039.

369

370 Amari, A., Gannouni, H., Khan, M. I., Almesfer, M. K., Elkhaleefa, A. M., Gannouni, A.(2018).  
371 Effect of structure and chemical activation on the adsorption properties of green clay mineral for the  
372 removal of cationic dye, *Appli Sci.*, 8, 2302-2320 .

373

374 Aysegul, A., Aynur,Ç., Yasemin, B., Zubeyde, B., & Çetin, A. (2013). Removal of methylene blue  
375 from aqueous solutions onto *Bacillus subtilis*: determination of kinetic and equilibrium parameters,  
376 *Desal. Water. Treat.*, 51, 7596- 7603.

377

378 Baghdadadi, M., Soltani, B. A., Nourani, M. (2017). Malachite green removal from aqueous solutions  
379 using fibrous cellulose sulfate prepared from medical cotton waste: Comprehensive batch and column  
380 studies, *J. Indust. Engine. Chemis.*, 55, 128-139.

381

382 Barka, N., Qourzal, S., Assabbane, A., Nounah, A., & Ait Ichou, Y. (2008). Adsorption of disperse  
383 blue SBL dye by synthesized poorly crystalline hydroxylapatite, *J. Environ. Scien.*, 20, 1268-1278.

384

385 Benguella, B., Nour, A. Y. (2009). Elimination des colorants acides en solution aqueuse par la  
386 bentonite et le kaolin, *C. R.Chimi.*, 12, 762-771.

387 Bentahar, S., Dbik, A., El Khomri, M., El Messaoudi, N., Lacherai, A. (2018). Removal of cationic  
388 dye from aqueous solution by natural clay, *Grou for Sust Develp.*, 6, 255-262.

389

390 Boukhemkhem, A., Rida, K. (2017). Improvement adsorption capacity of methylene blue onto  
391 modified tamazert kaolin, *Adsor Sci & Tech.*, 35, 753-773.

392

393 Chen, J., Lu, J., Su, L., H. Ruan, Zhao, Y., Lee, C., Cai, Z., Wu, Z., Jiang, Y. (2022). Enhanced  
394 Adsorption of Methyl Orange by Mongolian Montmorillonite after Aluminum Pillaring, *Appl. Sci.*,  
395 12, 3182.

396

397 Elaziouti, A., Laouedj, N., Bekka, A. (2011). Effect of pH Solution on the Optical Properties of  
398 Cationic Dyes in Dye/ Maghnia Montmorillonite Suspensions, *J. Chem. Eng. Process. Technol.*, 2,  
399 1-5

400 Gong, J., Pu, W., & Zhang, J. (2011). Liquid Phase De-position of Tungsten Doped TiO<sub>2</sub> Films for  
401 Visible Light Photoelectrocatalytic Degradation of Dodecyl Benzene-sulfonate, *Chemi Engine. J.*,  
402 67, 190-197.

403

404 Guiza, S., Bagane, M. (2013). Étude cinétique de l'adsorption du rouge de Congo sur une bentonite,  
405 R. Scie. Eau., 26, 39-51.

406

407 Hu, Z-P., Gao, Z-M., Liu, X., Yuan, Z-Y. (2018). High-surface-area activated red mud for efficient  
408 removal of methylene blue from wastewater, Adsor Sci & Tech., 36, 62-79.

409

410 Imene, F., Zoubida, T., Amina, R., Hayat, H., Safia, T. (2019). Discoloration of contaminated water  
411 by an industrial dye: Methylene Blue, by two Algerian bentonites, thermally activated, Alger. J.  
412 Environ. Scien. Techno., 1141-1148.

413 Kausar, A., Iqbal, M., Javed, A., Aftab, K., Nazli, Z. H., Bhatti, H. N., Nouren, S. (2018). Dyes  
414 adsorption using clay and modified clay: A Review, J of Mole Liqui., 256, 395-407.

415

416 Khan, M. I., Almesfer, M. K., Danish, M. I., Ali, H., Shoukry, Patel, H. R., Gardy, J. A., Nizami,  
417 S. M. (2019). Rehan, Potential of Saudi natural clay as an effective adsorbent in heavy metals  
418 removal from wastewater, Desal and Water Treat., 140–151.

419 Kumar, R., Singh, P., & Sharma, A. (2023). Efficient removal of glyphosate from aqueous solution  
420 using natural and modified clays: Kinetics and isotherm studies, Environ. Resea., 216, 114512.

421 Lunhong, A., You, Z., & Jiang, J. (2011). Removal of methylene blue from aqueous solution by  
422 montmorillonite / CoFe<sub>2</sub>O<sub>4</sub> composite with magnetic separation performance, Desal. 266, 72-77.

423

424 Magda, A., Mirian, C., Jardel, G., Gabriel, T., Cleuzir, D.L., Adriana, D., (2026). Novel eggshell-  
425 based pelletized adsorbent for glyphosate removal in batch reactor and fixed-bed column, Jou. of  
426 Mole. Liq. 442, 129074.

427

428 Maldonado, M., Gern Jak, Oller, W. I., Domenech, X. Peral, J. (2006). Partial Dégradation of five  
429 Pesticides and an Industrial Polluant by Ozonation in a pilot-plant Scale Reactor, J. HAZAR. Mater.,  
430 38, 363-369.

431

432 Mansour, H., Boughzala, B., Dridi, O. D., Darillier, D., Chekir-Ghedira, L., Mosrati, R. (2011). Les  
433 colorantes textiles sources de contamination de l'eau : CRIBLAGE de la toxicité et des méthodes de  
434 traitement, R. Scie. Eau., 24, 209-238.

435

436 Medjdoubi, Z., Hachemaoui, M., Boukoussa, B., Hakiki, A., Bengueddach, A., Hamacha, R. (2019).  
437 Adsorption behavior of janus green B dye on Algerian diatomite, Mater Resea Exp., 336-348.

438

439 Mekatel, A., Amokrane, A.S., Aid, A., Nibou, D., Trari, M. (2015). Adsorption of methyl orange on  
440 nanoparticles of a synthetic zeolite NaA/CuO, C.R.Chimi., 18, 336-344.

441

442 Mouni, L., Belkhiri, L., Bollinger, J-C., Bouzaza, A., Assadi, A., Tirri, A., Dahmoune, F., Madani,  
443 K., Remini, H. ( 2018). Removal of methylene blue from aqueous solutions by adsorption onto  
444 kaolin: kinetic and equilibrium studies, App Clay Scie., 153, 38-45.

445

446 Ngulube, T., Gumbo, J. R., Masindi, V., Maity, A. (2017). An update on synthetic dyes adsorption  
447 onto clay based minerals: A state-of-art review, J of Enviro Manag., 191, 35-57.

448

449 Omer, O. S., Hussein, M. A., Hussein, B. H., Mgaidi, A. (2018). Adsorption thermodynamics of  
450 cationic dyes (methylene blue crystal violet) to a natural clay mineral from aqueous solution between  
451 293.15 and 323.15 K, Arab Jour of Chemi., 11, 615-623.

452 Osama, Y., Saheed, A., Rakeen, M., (2025). Comparative Studies of regeneration and single Batch  
453 Design for the properties of basicblue-41removal using porous clay and porous acid activated  
454 heterostuctures, water. 17 (1) 2.

455 Organisation mondiale de la santé (OMS). Glyphosate critères de la qualité sanitaire de  
456 l'environnement, Programme international de sécurité des produits chimiques (IPCS), Genève.

457

458 Rytwo, G., Mendelovits, A., Eliyahu, D., Pitcovski, J. E. (2010). Aizenshtein, Adsoption of two  
459 vaccine-related proteins to montmorillonite and organo-montmorillonite, Appl.C.Scie., 50, 569-575.

460 Sabiha, E.K., Nese, T., Melike, F.D. (2025). Determination of glyphosate with a novel optic  
461 membrane sensor, Foo.Chemi., 475, 143361.

462 Sabrine, B., J. A, C., Nesrine, C., Vilarrasa-García, E., Rodríguez-Castellón, E., Mohamed, C.,  
463 Mohamed, B., (2022). Glyphosate adsorption onto porous clay heterostructure (PCH): kinetic and  
464 thermodynamic studies, Brazi.Jour.of Chem. Engi, 39, 903-917.

465

466 Şahin, Ö., Kaya, M., Saka, C. ( 2015). Plasma-surface modification on bentonite clay to improve the  
467 performance of adsorption of methylene blue, Appl Clay Sci., 116 , 46-53.

468

469 Sarma, G. K., SenGupta, S., Bhattacharyya, K. G. (2011). Methylene blue adsorption on natural and  
470 modified clays, Sep Sci and Techn., 46, 1602-1614.

471

472 Ugurlu, M.,& Karaoglu M. H. (2011). TiO<sub>2</sub> Supported on Sepolite: Preparation, Structural and  
473 Thermal Characterization and Catalytic Behaviour in Photocatalytic Treatment of Phenol and Lignin  
474 from Olive Mill Wastewater, Chemi. Engine. J., 166, 859-867.

475

476 Youcef, Z. D., Bouabdasselem, H., Bettahar, N. (2006). Élimination des composés organiques par  
477 des argiles locales, C. R. Chimi., 9, 1295-1300.

478

479 Yudha, G. W., Hana, S., Kholivia, C., Arif, R., Sudiby, A. T. Y., Himawan, T. B. M., Setyo, B.,  
480 Bimastyaji S. R., Anis, T. M., Hutwan, S. (2025). Enhanced modified Magnetite Bentonite-  
481 CaO/FeCl<sub>3</sub> from solid waste for highly efficient Methylene blue removal, 26, 4.

482

483 Zhang, L., Mi, M., Li, B., Dong, Y. (2013). Modification of activated carbon using microwave heating  
484 and its effects on the pore texture and surface chemistry, Res. J. Appl. Sci. Eng. Technol. 1836–1840.

ACCEPTED MANUSCRIPT